

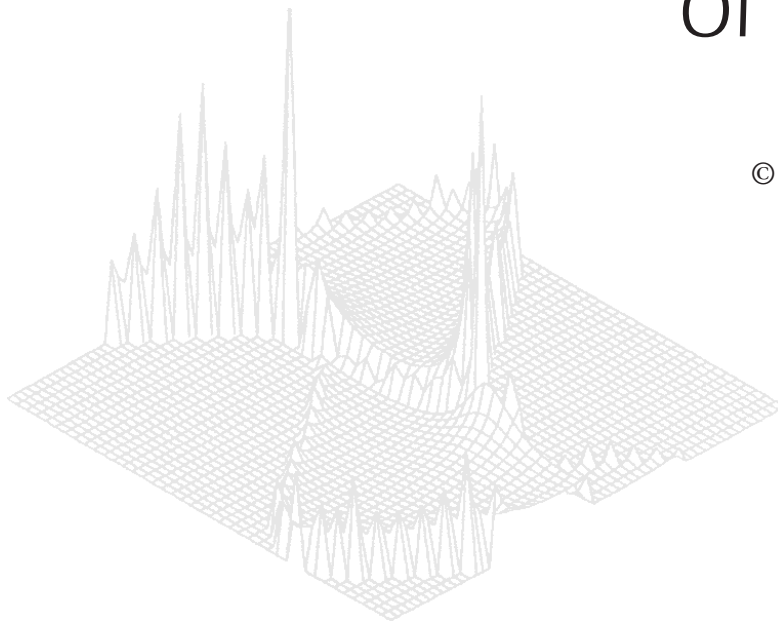
---

**C S I R O   P U B L I S H I N G**

---

# Australian Journal of Physics

Volume 50, 1997  
© CSIRO Australia 1997



A journal for the publication of  
original research in all branches of physics

**[www.publish.csiro.au/journals/ajp](http://www.publish.csiro.au/journals/ajp)**

All enquiries and manuscripts should be directed to

*Australian Journal of Physics*

**CSIRO PUBLISHING**

PO Box 1139 (150 Oxford St)

Collingwood

Vic. 3066

Australia

Telephone: 61 3 9662 7626

Facsimile: 61 3 9662 7611

Email: [peter.robertson@publish.csiro.au](mailto:peter.robertson@publish.csiro.au)



Published by **CSIRO PUBLISHING**  
for CSIRO Australia and  
the Australian Academy of Science



## Ion Confinement in a Toroidal Helic

*J. L. V. Lewandowski*

Research School of Physical Sciences and Engineering, Plasma Research Laboratory and,  
Department of Theoretical Physics, Australian National University,  
Canberra, ACT 0200, Australia.

### *Abstract*

A model to describe an unmagnetised plasma in three-dimensional magnetic topology is presented. Ion trajectories are integrated numerically and all finite-Larmor radius effects are retained exactly. A velocity-dependent collision term is included in the equations of motion. Numerical simulations relevant to the low-confinement mode of H1-NF are presented and discussed.

### 1. Introduction

A high-confinement mode has been recently observed in the toroidal heliac H1-NF (Shats *et al.* 1996). An improvement in the energy and particle confinement times has been observed when the input heating power  $P$  is above the threshold  $P^*$ . Improved confinement is associated with an increase in the (negative) radial electric field near the plasma edge. Experimental observations suggest that the power threshold depends (1) on the magnetic field strength and (2) on the rotational transform of the confining magnetic field (Shats *et al.* 1996). Typical plasma parameters for these experiments are  $n \sim 10^{11} \text{ cm}^{-3}$ ,  $T_i \sim 40 - 90 \text{ eV}$ ,  $m_i/m_p = 40$  (where  $m_p$  is the proton mass),  $T_e \sim 15 \text{ eV}$  and  $B \sim 10^{-1} \text{ T}$ .

The plasma magnetisation is described by the parameter  $\delta_i \equiv \rho_i/\bar{a}$ , where  $\rho_i$  is the ion thermal gyro-radius and  $\bar{a}$  is the average major radius of the configuration. A magnetised plasma satisfies  $\delta_i/\bar{a} \ll 1$  (Hazeltine and Meiss 1992). With the above plasma parameters the ion population is unmagnetised (i.e.  $\delta_i \sim 1$ ) in the bulk of the plasma. Fluid (Braginskii 1965; Drake and Antonsen 1984), gyro-kinetic (Rewoldt and Chen 1982; Antonsen and Lane 1980) and drift-kinetic (Hazeltine 1973) models rely on the assumption of a magnetised plasma. Such models are *a priori* not valid to describe H1-NF plasma with the above parameters since higher order corrections in  $\delta_i$  are not small.

In this paper we consider an unmagnetised plasma in fully 3D geometry. The equation of motion of a set of ions is integrated numerically. Collisional effects are taken into account. The fully 3D nature of the confining magnetic field is retained so that corrections of all orders in  $\delta_i$  are treated exactly.

The paper is organised as follows. In Section 2, we specify the equilibrium magnetic field for the H1-NF configuration. In Section 3, a model describing the ion population is presented. A velocity-dependent collision term is included in

the ion motion equation. Numerical results for the H1-NF plasma are presented in Section 4.

## 2. The Equilibrium

The equilibrium magnetic field is determined numerically using the VMEC code (Hirshman and Whitson 1983; Hirshman and Meier 1985; Hirshman and Lee 1986) from the ideal MHD force balance equation

$$\mathbf{J} \times \mathbf{B} = c \nabla p_0, \quad (1)$$

where  $\mathbf{J}$  is the current density and  $p_0$  is the plasma pressure. The current density in (1) is computed from Ampere's law,

$$4\pi \mathbf{J} = c \nabla \times \mathbf{B}. \quad (2)$$

Equations (1) and (2) are supplemented with the divergence-free condition  $\nabla \cdot \mathbf{B} = 0$ . Equilibrium magnetic surfaces are assumed to form a family of nested torii. For 3D stellarator equilibria it is convenient to write the magnetic field in curvilinear coordinates  $(s, \theta, \phi)$ , where  $s \equiv \Psi/\Psi_b$  is the radial label,  $\theta$  is an optimised poloidal angle (determined so that the numerical convergence is improved) and  $\phi$  is the usual azimuthal angle in cylindrical coordinates (Hirshman and Betancourt 1991). Here  $\Psi$  is the enclosed toroidal flux and  $\Psi_b$  is its corresponding value evaluated at the plasma boundary. By construction the radial label  $s$  runs from 0 (at the magnetic axis) to 1 (at the plasma boundary). The existence of magnetic surfaces implies  $\mathbf{B} \cdot \nabla s = 0$ . In these coordinates, the magnetic field can be written in terms of the covariant basis vectors

$$\mathbf{B} = B^\theta \mathbf{e}_\theta + B^\phi \mathbf{e}_\phi, \quad (3)$$

where the covariant basis is defined as  $\mathbf{e}_\theta \equiv \partial \mathbf{r}_*/\partial \theta$  and  $\mathbf{e}_\phi \equiv \partial \mathbf{r}_*/\partial \phi$  and where  $\mathbf{r}_*$  is the local position vector on a magnetic surface. We have made use of the assumption of the existence of nested magnetic surfaces,  $\mathbf{B} \cdot \nabla s = 0$ . In equation (3)  $B^\theta \equiv \mathbf{B} \cdot \nabla \theta$  and  $B^\phi \equiv \mathbf{B} \cdot \nabla \phi$ , where the contravariant basis vectors are defined as  $\nabla i = \mathcal{J}^{-1} \epsilon_{ijk} (\mathbf{e}_j \times \mathbf{e}_k)$ , for  $(i, j, k) = \{s, \theta, \phi\}$ , where  $\mathcal{J} = \mathbf{e}_s \cdot (\mathbf{e}_\theta \times \mathbf{e}_\phi)$  is the Jacobian of the transformation and  $\epsilon_{ijk}$  is the usual Levi-Civita symbol for permutations (D'haeseleer *et al.* 1991). In these coordinates the Jacobian of the transformation scales like a volume. The magnetic field can alternatively be written as a linear combination of the contravariant basis vectors

$$\mathbf{B} = B_s \nabla s + B_\theta \nabla \theta + B_\phi \nabla \phi, \quad (4)$$

where  $B_s \equiv \mathbf{B} \cdot \mathbf{e}_s$ ,  $B_\theta \equiv \mathbf{B} \cdot \mathbf{e}_\theta$  and  $B_\phi \equiv \mathbf{B} \cdot \mathbf{e}_\phi$ . The VMEC code (Hirshman and Whitson 1983; Hirshman and Meier 1985; Hirshman and Lee 1986) outputs the position and shape of the magnetic surfaces in cylindrical coordinates  $(R, Z, \phi)$ . In particular the coordinates  $R$  and  $Z$  are specified in terms of Fourier series,

$$R = \sum_{m=0}^M \sum_{n=-N}^{n=+N} \cos(\mu_{mn}), \quad Z = \sum_{m=0}^M \sum_{n=-N}^{n=+N} \sin(\mu_{mn}), \quad (5)$$

for a given magnetic surface. Here  $\mu_{mn} \equiv m\theta + N_{\text{per}}n\phi$  and  $N_{\text{per}}$  is the number of field periods. For H1-NF,  $N_{\text{per}} = 3$ . The number of poloidal ( $M$ ) and toroidal ( $N$ ) Fourier components describing the equilibrium can be varied until a given level of accuracy is reached (or depending on the complexity of the magnetic configuration). The choice  $M = 7$  and  $N = 14$  has been used in this paper. In order to retain all finite-Larmor radius (FLR) effects with good accuracy the number of magnetic surfaces ( $=N_s$ ) describing the equilibrium must be chosen to be relatively large. Therefore we have chosen  $N_s = 100$ .

The curvilinear components of the magnetic field are given in terms of Fourier series similar to equation (5). The equilibrium electron and ion temperatures ( $T_e$  and  $T_i$  respectively) and the plasma density  $n$  are assumed to be flux surface quantities, i.e. to depend on  $s$  only.

### 3. The Model

As we briefly discussed in the Introduction the plasma magnetisation parameter  $\delta_i$  is of the order of unity for H1-NF plasma conditions (Shats *et al.* 1997). Fluid, gyro-kinetic and drift-kinetic models make use of the fact that  $\delta_i \ll 1$ . Fluid and drift-kinetic models neglect corrections of  $\mathcal{O}(\delta_i)$ , but the gyro-kinetic model takes into account terms of  $\mathcal{O}(\delta_i)$ . Such models are *a priori* not valid to describe the ion population in the H1 argon plasma because corrections of order  $\mathcal{O}(\delta_i^2)$  and higher can be important.

For example the ion velocity, in the guiding centre approximation, reads (see for instance Hazeltine and Meiss 1992)

$$\mathbf{v}_{\text{gci}} = \frac{c}{B} (\mathbf{E} \times \mathbf{e}_{\parallel}) + \frac{v_{\parallel}^2}{\omega_{\text{ci}}} (\mathbf{e}_{\parallel} \times \boldsymbol{\kappa}) + \frac{v_{\perp}^2}{2\omega_{\text{ci}}} \left( \mathbf{e}_{\parallel} \times \frac{\nabla B}{B} \right), \quad (6)$$

where, for a low- $\beta$  plasma, the electric field is derivable from an electrostatic potential  $\mathbf{E} = -\nabla\Phi$ ,  $\mathbf{e}_{\parallel} \equiv \mathbf{B}/B$  is a unit vector parallel to the magnetic field direction,  $\boldsymbol{\kappa} \equiv \mathbf{e}_{\parallel} \cdot \nabla \mathbf{e}_{\parallel}$  is the magnetic field curvature and  $\omega_{\text{ci}} \equiv q_i B / m_i c$  is the gyro-frequency for the ions. To lowest order in  $\rho_i / \bar{a}$ , ions and electrons drift across the magnetic surface with the same velocity  $\mathbf{v}_e = c(\mathbf{E} \times \mathbf{e}_{\parallel})/B$ . The last two terms in equation (6) are of the same order  $\sim V_{\text{thi}}\delta_i$ , where  $V_{\text{thi}}$  is the ion thermal velocity. As we previously pointed out we consider an unmagnetised plasma so that  $\delta_i$  is formally of the order of unity. In this case corrections of  $\mathcal{O}(\delta_i^2)$  and higher can substantially modify the ion guiding-centre velocity (6). Corrections of order  $\delta_i^2$  involve the manipulation of tensorial quantities for the confining magnetic field. In curvilinear coordinates the explicit calculations of such quantities becomes rapidly complicated, the degree of complexity increasing sharply for  $p \geq 2$  for corrections  $\mathcal{O}(\delta_i^p)$ .

For electrons the curvature drift can be safely neglected so that  $\mathbf{v}_{\text{gce}} = \mathbf{v}_e + \mathcal{O}(V_{\text{the}}m_e/m_i) \approx \mathbf{v}_e$  ( $V_{\text{the}}$  is the electron thermal velocity). The electron population is magnetised.

In order to retain the effects of the magnetic field inhomogeneity to *all* orders in  $\rho_i / \bar{a}$  one has to numerically integrate the equation of motion for the ions:

$$m_i \frac{d\mathbf{V}_i}{dt} = Z_i e \left( \mathbf{E} + \frac{\mathbf{V}_i \times \mathbf{B}}{c} \right) + \sum_{j \neq i} \mathbf{F}_{ij} + \mathbf{F}_h, \quad (7)$$

where  $\mathbf{E}$  and  $\mathbf{B}$  are the equilibrium electric and magnetic fields respectively,  $Z_i$  is the ion charge and  $\mathbf{F}_h$  represents the force on the ions due to the heating system. The timescale of the heating force is  $F_h^{-1} \partial F_h / \partial t \sim \omega_h$ , where  $\omega_h$  is the rf heating frequency. The force induced by a fluctuating electric field, presumably generated by unstable drift waves (Shats *et al.* 1996), will be entirely neglected. The first term on the right-hand side of equation (7) is the usual Lorentz force. The second term represents the transfer of momentum to ion species  $i$  due to collisions with ion species  $j$ . Following Trubnikov (1965) the collisional momentum transfer can be written as  $\mathbf{F}_{ij} = -m_i \mathbf{V}_i / \tau_{ij}$  where  $\tau_{ij}$  is the average deflection time given by

$$\tau_{ij} = \frac{4\pi V_1^3}{(1 + m_i/m_j) n_j L_{ij} f(y)}, \quad (8)$$

where  $L_{ij} \equiv \Lambda(4\pi e^2 Z_i Z_j)^2 / m_i^2$ ;  $y \equiv m_j V_i^2 / 2T_j$  is the kinetic energy for ion species  $i$  normalised to the ion temperature for species  $j$ ; and  $f(x) \equiv 2 \int_0^x \exp(-t) \sqrt{t} dt / \sqrt{\pi}$  is the so-called Maxwell integral (Spitzer 1956). Let  $\tau_{ij}^{(0)} \equiv (4\pi V_{\text{thi}0}^3) / [(1 + m_i/m_j) n_j L_{ij} f(1)]$ , where  $V_{\text{thi}0}$  is the ion thermal velocity evaluated at the magnetic axis, so that the collision term may be rewritten as

$$\sum_{j \neq i} \mathbf{F}_{ij} = -\frac{m_i V_{\text{thi}0}}{\bar{\tau}_i} \frac{\mathbf{v}_i}{v_i^3} G(v_i), \quad (9)$$

where  $\mathbf{v}_i \equiv \mathbf{V}_i / V_{\text{thi}0}$  is the normalised ion velocity and  $\bar{\tau}_i^{-1} \equiv \sum_{j \neq i} 1 / \tau_{ij}^{(0)}$ . We have defined  $G(v_i) \equiv f(v_i^2) / f(1)$  where  $f(1) \simeq 0.4276$  is a constant. We have assumed  $T_i / T_j \simeq 1$ .

The conservation of kinetic energy for  $i - j$  collisions is

$$\frac{1}{2} m_i v_i^2 + \frac{1}{2} m_j v_j^2 = \frac{1}{2} m_i v_i^{*2} + \frac{1}{2} m_j v_j^{*2}, \quad (10)$$

where  $v_i^*$  and  $v_j^*$  are the ion velocities (for species  $i$  and  $j$  respectively) after the collision. Formally one has to consider all possible  $i - j$  collisions; however this approach would require the simultaneous solution of  $\sim \sum_j N_j$  equations of motions, where  $N_j$  is the prescribed number of ions for species  $j$ . For practical applications, the limits set by computer speed and memory do not allow the simultaneous solution of such a system. For simplicity we shall assume that the ion  $i$  interacts with the bulk of ions of species  $j$ . Operating with  $n_j^{-1} \int \dots f_j dv$  on equation (10), where  $n_j$  and  $f_j$  are the density and distribution function for species  $j$ , leads to  $v_j^2 = v_i^{*2}$ , i.e. the kinetic energy for species  $i$  is conserved in the average sense. The change in *direction* for the ion velocity can be written as

$$\begin{aligned} \mathbf{v}_i \text{ (before collision)} &\mapsto \frac{v_i}{\xi} [(\xi_1 - \frac{1}{2}) \hat{\mathbf{x}} + (\xi_2 - \frac{1}{2}) \hat{\mathbf{y}} \\ &+ (\xi_3 - \frac{1}{2}) \hat{\mathbf{z}}] \text{ (after collision)}, \end{aligned} \quad (11)$$

where  $\xi_1, \xi_2$  and  $\xi_3$  are random numbers between 0 and 1. Here  $(\hat{\mathbf{x}}, \hat{\mathbf{y}}, \hat{\mathbf{z}})$  are unit vectors in Cartesian coordinates. Since the kinetic energy for ion  $i$  is conserved (in the average sense) this implies that  $\xi = [(\xi_1 - \frac{1}{2})^2 + (\xi_2 - \frac{1}{2})^2 + (\xi_3 - \frac{1}{2})^2]^{\frac{1}{2}}$ .

The heating system induces an oscillating (parallel) electric field with frequency  $\omega_h$  much larger than the ion gyro-frequency. The parallel component of the ion velocity induced by the heating system is approximately given by  $V_{i\parallel} \approx V_{\text{thi}} \cos(\omega_h t + \varphi)$  where  $\varphi$  is an arbitrary phase. The ion momentum equation (7) will be numerically integrated with a time step  $\Delta t \omega_{ci} \ll 1$ . For a time step not too short,  $\Delta t \omega_h \gg 1$ , the change in the parallel ion velocity due to the rf-induced parallel electric field during  $\Delta t$  is negligible compared to the change in its perpendicular component,

$$\Delta V_{i\parallel} \equiv \frac{1}{\Delta t} \int_0^{\Delta t} V_{i\parallel}(t') dt' \ll \Delta V_{i\perp}. \quad (12)$$

Therefore, as long as the condition  $\Delta t \omega_h \gg 1$  is satisfied, the interaction of the heating system with the ion dynamics can be safely neglected.

The (equilibrium) electrostatic potential is assumed to be a flux surface quantity  $\Phi = \Phi(s)$  so that the confining electric field reads  $\mathbf{E} = -d\Phi/ds \nabla s$ . Neglecting the rapid, oscillating parallel ion motion due to the heating system, the Cartesian components of the ion equation of motion are:

$$\begin{aligned} \frac{dv_{ix}}{dt''} &= -P \frac{d\tilde{\Phi}}{ds} C_x + b_z v_{iy} - b_y v_{iz} - \frac{G(v_i)(\xi_1 - \frac{1}{2})}{\bar{\xi} \mathcal{M} v_i^2} \\ \frac{dv_{iy}}{dt''} &= -P \frac{d\tilde{\Phi}}{ds} C_y + b_x v_{iz} - b_z v_{ix} - \frac{G(v_i)(\xi_2 - \frac{1}{2})}{\bar{\xi} \mathcal{M} v_i^2}, \\ \frac{dv_{iz}}{dt''} &= -P \frac{d\tilde{\Phi}}{ds} C_z + b_y v_{ix} - b_x v_{iy} - \frac{G(v_i)(\xi_3 - \frac{1}{2})}{\bar{\xi} \mathcal{M} v_i^2}. \end{aligned} \quad (13)$$

In the last term of each equation, we note that  $v_i^2 = v_{ix}^2 + v_{iy}^2 + v_{iz}^2$ . Here we have introduced the normalised magnetic field  $\mathbf{b} \equiv \mathbf{B}/B_0 \sim 1$  (where  $B_0$  is the magnetic field strength at the magnetic axis),  $t'' \equiv \omega_{ci0} t$  is the normalised time,  $\tilde{\Phi} \equiv e\Phi/T_{i0}$  is the normalised electrostatic potential,  $P \equiv (m_i c T_{i0} V_{\text{thi0}})/(2\bar{a}eB_0)$ ,  $\mathbf{C} \equiv \bar{a}\nabla s$  is a nondimensional quantity describing the noncircularity of the magnetic surface, and  $\mathcal{M}(s) \equiv \omega_{ci0} \bar{\tau}_i$  is a nondimensional parameter related to the plasma collisionality.

For an almost collisionless plasma,  $\mathcal{M} \gg 1$ , the last terms in equations (13) can be neglected. The resulting equations describe the ion motion in the presence of an accelerating (or decelerating) electric field and an inhomogeneous magnetic field  $\nabla B \neq 0$ . All the quantities  $b_x, b_y$  and  $b_z$  are evaluated at the particle position  $\mathbf{r}_i$ . Therefore, corrections of *all* orders in  $\rho_i/\bar{a}$  are retained exactly.

The parameter  $\mathcal{M}$  depends on the density of the ion species  $j$  as well as the kinetic energy for the ion species  $i$  through the Maxwell integral. Shats *et al.* (1997) have suggested that, for H1-NF plasma conditions, a coronal model can be used to determine the ionisation balance. It was also pointed out that ions with  $Z_i = 1, 2, 3$  can be simultaneously present in an H1-NF argon plasma (Shats *et al.* 1997). For a low magnetic field the ions assume a Boltzmann distribution in the electrostatic potential,

$$n_j = n_{e0} D_j \exp(-Z_j \Delta \tilde{\Phi}), \quad (14)$$

where  $n_{e0}$  is the electron density at the magnetic axis;  $D_j$  is the fraction of ions with charge  $Z_j$ ; and  $\Delta \tilde{\Phi} \equiv \tilde{\Phi}(s) - \tilde{\Phi}(0)$  is the difference between the normalised electrostatic potential  $\tilde{\Phi}(s) \equiv e\Phi(s)/T_{i0}$  at the radial position  $s$  and its value evaluated at the magnetic axis. The coefficients  $D_j$  were obtained by using a fit to the experimental data for the quasineutrality condition. Shats *et al.* (1997) have found  $D_1 = 0.2$ ,  $D_2 = 0.4$  and  $D_3 = 0.4$  for the argon species  $Ar^+$ ,  $Ar^{++}$  and  $Ar^{+++}$  respectively.

It is worth noting that for ions with low velocity,  $v_i \leq 1$ , the collision term is important because of the  $V_i^{-3}$  dependence of the Coulomb collision term. This effect is increased in the region for which the collisional parameter becomes of order unity. In the low-confinement mode the electrostatic potential increase monotonically from the magnetic axis ( $s = 0$ ) to the plasma edge ( $s = 1$ ). The high- $Z_i$  ions therefore tend to ‘accumulate’ in the plasma centre. The average deflection time (8) is strongly dependent on the charge number,  $\tau_{ij} \propto Z_j^{-2} \exp(Z_j \Delta \tilde{\Phi})$ . As it turns out the collision parameter is of the order unity at the magnetic axis and increases by a factor  $\sim 20$  at the plasma edge. The parameter  $P$  for the radial electric field is of the order unity. In particular in the low-confinement of H1-NF with  $B_0 \simeq 0.06$  T,  $T_{i0} \simeq 40$  eV,  $\bar{a} \simeq 12$  cm,  $Z = 1$  and  $\tilde{\Phi} \simeq 1$ , we find  $P \simeq 0.3$ . Therefore the electric and magnetic terms in equation (13) are of comparable magnitude.

Equations (13) are supplemented with

$$\frac{dx_i}{dt''} = v_{ix}, \quad \frac{dy_i}{dt''} = v_{iy}, \quad \frac{dz_i}{dt''} = v_{iz}, \quad (15)$$

where  $x_i$ ,  $y_i$  and  $z_i$  are the  $x$ ,  $y$  and  $z$  components of the position vector  $\mathbf{r}$  normalised to the ion thermal gyro-radius evaluated at the magnetic axis,  $\rho_{i0} = V_{thi0}/\omega_{ci0}$ . The numerical solution of equations (13) and (15) is discussed in the next section.

#### 4. Numerical Simulations and Discussion

Equations (13) and (15) have been integrated numerically with a fifth-order Runge–Kutta method (Press *et al.* 1983). All the physical quantities depending on the magnetic field topology ( $b_x, b_y, b_z, C_x, C_y$  and  $C_z$ ) are evaluated on a discrete grid. For example, the  $x$  component of the normalised magnetic field is computed at each grid point  $b_x^{[tmp]} \equiv b_x(s_t, \theta_m, \phi_p)$ , where  $t = 1, \dots, N_s$  labels the magnetic surface,  $\theta_m = (m - \frac{1}{2})\Delta\theta$  for  $m = 1, \dots, N_\theta$  and  $\phi_p = (p - \frac{1}{2})\Delta\phi$  for  $p = 1, \dots, N_\phi$ . Here  $\Delta\theta_j \equiv 2\pi/N_\theta$  and  $\Delta\phi \equiv 2\pi/N_\phi$  are the mesh size in the poloidal and toroidal directions, respectively. At each time step and for each particle, the closest neighbour between the particle position  $\mathbf{r}_i^{[k]}$  ( $k$  labels the ion,  $k = 1, \dots, N_i$  where  $N_i$  is the number of ions) and the position vector  $\mathbf{r}_*(s_t, \theta_m, \phi_p)$ , defined on a magnetic surface, is determined.

The numbers  $N_\theta$  and  $N_\phi$  must be chosen sufficiently large so that the ion FLR effects can be treated accurately. In this paper we have used  $N_\theta = 70$  and  $N_\phi = 620$ . The normalised time step is taken to be  $\Delta t'' = \omega_{ci0} \Delta t = 5 \times 10^{-3}$ .

The curvature of the magnetic surface enters in equation (13) through the vector  $\mathbf{C}$ . From equation (5) the position vector on a magnetic surface can be written in cylindrical coordinates as  $\mathbf{r}_* = R \cos \phi \hat{\mathbf{x}} + R \sin \phi \hat{\mathbf{y}} + Z \hat{\mathbf{z}}$ . Making use of the relation  $\nabla s = \mathcal{J}^{-1}(\mathbf{e}_\theta \times \mathbf{e}_\phi)$  we can easily compute the Cartesian components of the vector  $\mathbf{C}$ . These components are:

$$\begin{aligned} C_x &= \bar{a} \mathcal{J}^{-1} [\sin \phi \partial_\phi Z \partial_\theta R - \partial_\theta Z (R \cos \phi - \sin \phi \partial_\phi R)], \\ C_y &= \bar{a} \mathcal{J}^{-1} [\sin \phi \partial_\theta R (\cos \phi \partial_\phi R - R \sin \phi) - \cos \phi \partial_\theta R \partial_\phi Z], \\ C_z &= \bar{a} \mathcal{J}^{-1} [\cos \phi \partial_\theta R (\sin \phi \partial_\phi R + R \cos \phi) \\ &\quad - \sin \phi \partial_\theta R (\cos \phi \partial_\phi R - R \sin \phi)], \end{aligned} \quad (16)$$

where  $\partial_\theta \equiv \partial/\partial\theta$  and  $\partial_\phi \equiv \partial/\partial\phi$ .

The (normalised) magnetic field strength on the magnetic surface  $s = 0.96$  of the toroidal heliac H1-NF is shown in Fig. 1. The regions of high magnetic field strength are indicated in white, while regions of low magnetic field strength are shown in black. The effects of the toroidal field coil ripples are clearly visible on the outside of the magnetic surface.

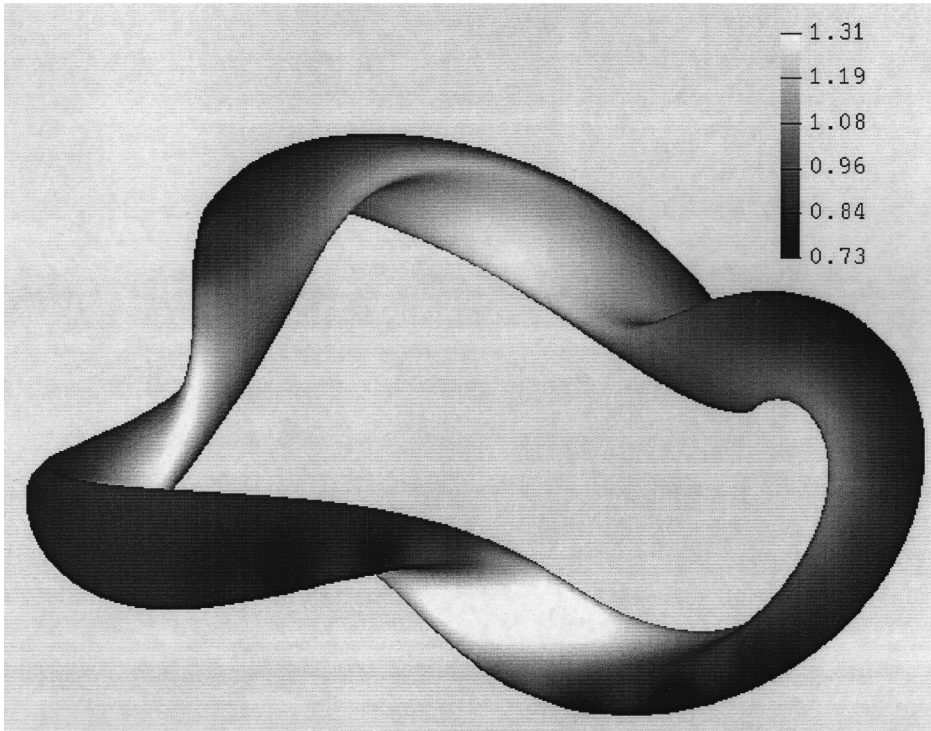


**Fig. 1.** Normalised magnetic field strength on a magnetic surface of the toroidal heliac H1-NF at  $s = 0.96$ . The shaded regions in black (white) correspond to low (high) magnetic field strength.

A poloidal cross section, at  $\phi = 0$ , for the same configuration as in Fig. 1, is shown in Fig. 2. For the sake of clarity a reduced set of 21 magnetic surfaces is shown. We note the characteristic ‘bean shape’ of the H1-NF plasma.

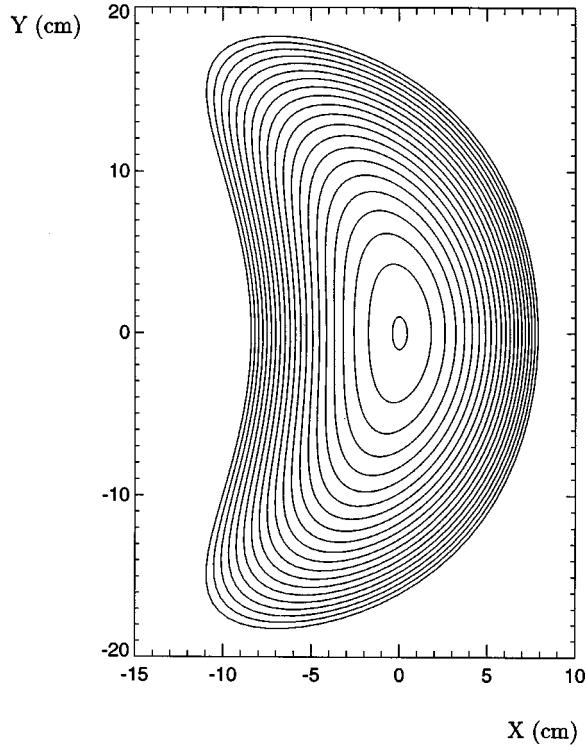


**Fig. 2.** Poloidal cross section of the H1-NF plasma at the plane  $\phi = 0$ . A set of 21 nested magnetic surfaces is shown.

At the beginning of the simulations the ions were randomly distributed along the magnetic axis ( $s = 0$ ). The trajectories of a set of  $N_i = 2 \times 10^3$   $Ar^+$  ions were integrated. At  $t = 0$  the ion distribution is assumed to be isotropic with a zero mean velocity. Specifically, at  $t = 0$ , the  $k^{\text{th}}$  ion has the following velocity components:

$$\begin{aligned} v_x^{[k]} &= v_0 \sin(2\pi\xi_1) \cos(2\pi\xi_2), \\ v_y^{[k]} &= v_0 \sin(2\pi\xi_1) \sin(2\pi\xi_2), \\ v_z^{[k]} &= v_0 \cos(2\pi\xi_1), \end{aligned} \quad (17)$$

where, as before,  $\xi_1$  and  $\xi_2$  are two random numbers between 0 and 1. We have chosen  $v_0 = 1.0$ .

Experimental measurements (Shats *et al.* 1996) indicate that the radial electric field changes sign at the last closed magnetic surface (defined as  $s = 1$ ). In the low-confinement mode the radial electric field becomes positive for  $s > 1$ , so that

the ions are pushed out of the plasma bulk. For simplicity we assume that ions satisfying  $s > 1$  are lost.

In order to study the effects of the magnetic field inhomogeneity, electric force and collisional force, we have considered two cases. In case A all the terms in equation (13) were retained; and in case B the collisional term ( $\mathcal{M} \mapsto \infty$ ) and the radial electric field were neglected.

The collisional parameters for  $Ar^+ - Ar^{++}$ ,  $Ar^+ - Ar^{+++}$  and  $Ar^+ - Ar^{++}/Ar^{+++}$  ( $= \mathcal{M}$ ) collisions are shown in Fig. 3. The mean collisional parameter (solid curve) increases by more than one order of magnitude from the magnetic axis ( $s = 0$ ) to the last closed magnetic surface ( $s = 1$ ). Therefore collisional effects can be important in the bulk of the plasma. Near  $s = 1$ , the plasma is almost collisionless.

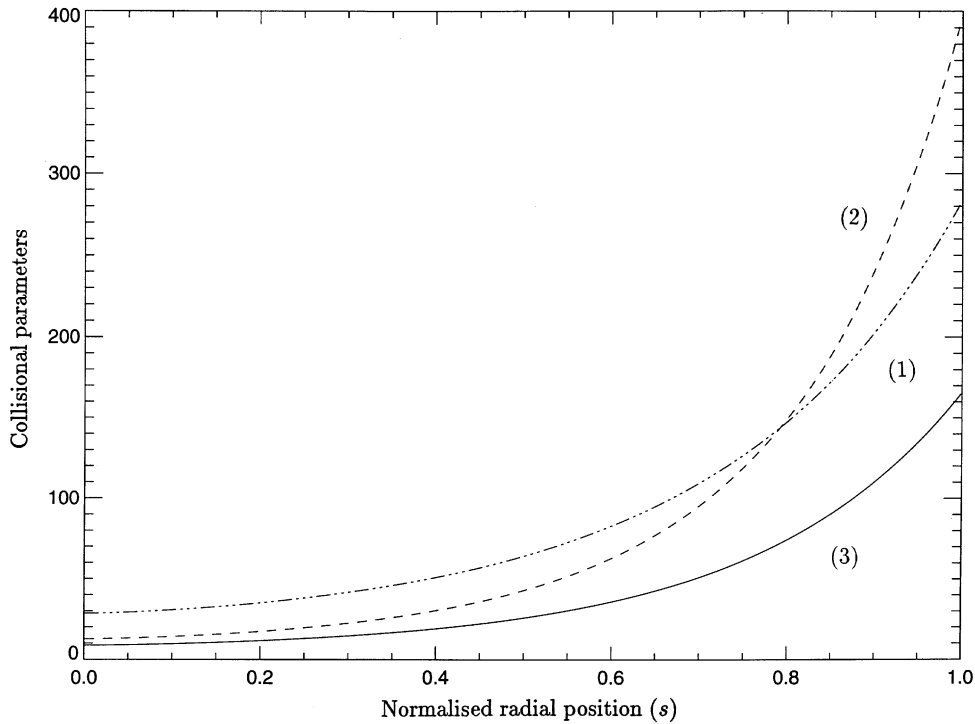


**Fig. 3.** Collisional parameters (1) for  $Ar^+ - Ar^{++}$  collisions, (2) for  $Ar^+ - Ar^{+++}$  collisions and (3) for  $Ar^+ - Ar^{++}/Ar^{+++}$  collisions as a function of the normalised radial label.

The fraction of confined ions as a function of the (normalised) time is shown in Fig. 4. The two profiles display different behaviours for  $t'' \geq 1.5$ . When collisional effects and the radial electric field are neglected (case B) the ions are continuously lost from the plasma bulk. In case A however, the fraction of confined ions indicates an asymptotic saturation. In this regime approximately  $\frac{1}{3}$  of the ions remain well confined.

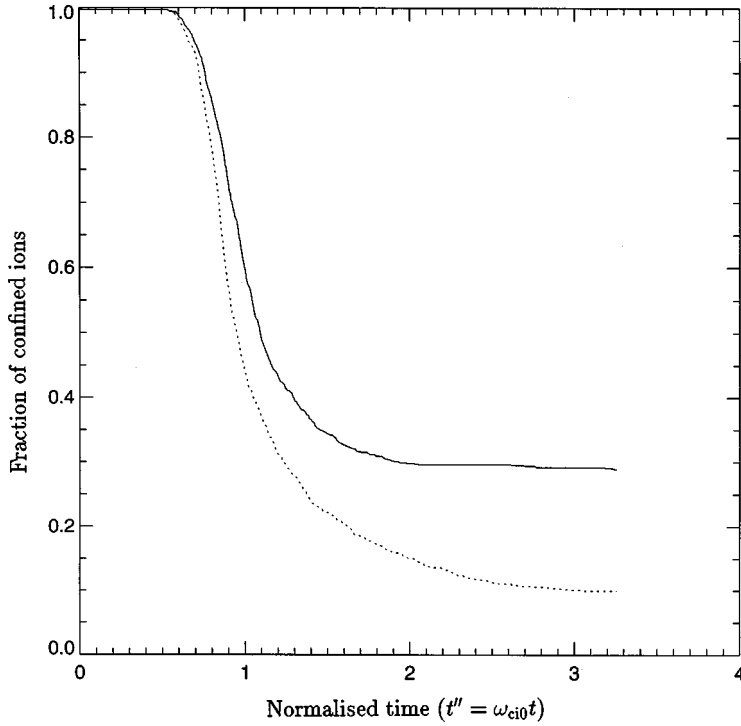


Fig. 4. Fraction of confined ions as a function of the normalised time  $t'' \equiv \omega_{ci}t$  for case A (solid curve) and for case B (dotted curve).

The average radial displacement defined as

$$\langle s(t'') \rangle \equiv \frac{1}{N_c(t'')} \sum_{k=1}^{N_c(t'')} s^{[k]}, \quad (18)$$

where  $N_c$  is the number of confined ions, is shown in Fig. 5. A transition at  $t'' \sim 1.5$  is clearly visible. In case A the average radial position of the ions decreases for  $t'' \geq 1.5$ , indicating good confinement properties of the configuration. In case B the average radial position saturates around  $s \simeq 0.25$ .

Finally we have computed the average velocity normal to a magnetic surface. The normal velocity is defined as

$$v_n \equiv \mathbf{v} \cdot \hat{\mathbf{n}}, \quad (19)$$

where  $\hat{\mathbf{n}} \equiv \nabla s / (\nabla s \cdot \nabla s)^{1/2}$  is a unit vector normal to the magnetic surface and pointing outwards. The average normal velocity  $\langle v_n \rangle$  is shown in Fig. 6. The normal velocity changes sign at  $t'' \simeq 1.6$  for case A and at  $t'' \simeq 3.0$  for case B. Therefore the *integrated* normal drift,

$$\bar{s}(t'') \equiv \bar{s}(0) + \int_0^{t''} \langle v_n \rangle(t) dt, \quad (20)$$

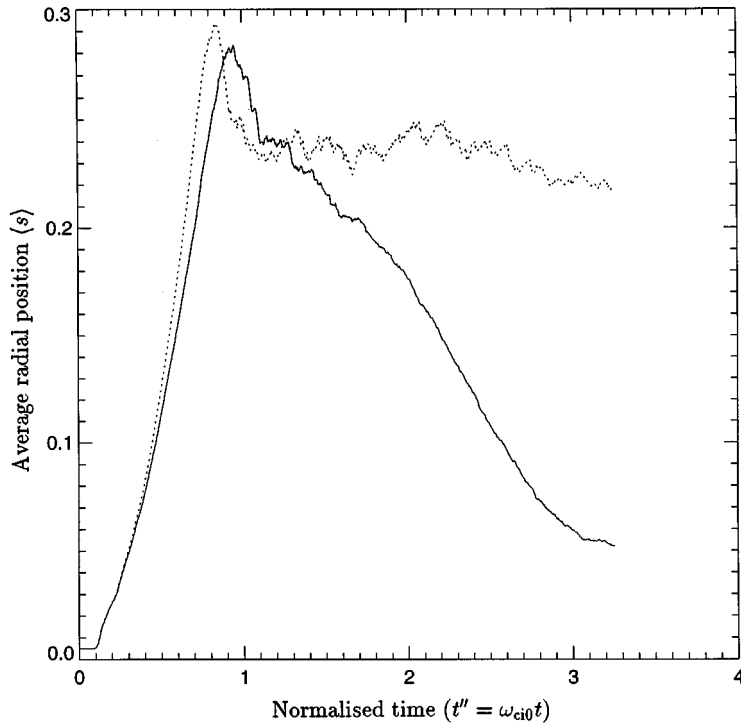


**Fig. 5.** Average radial position ( $s$ ) for the  $Ar^+$  ion population as a function of the normalised time for case A (solid curve) and for case B (dotted curve).

is smaller in case A than in case B. This is again the signature of improved ion confinement.

## 5. Concluding Remarks

In this paper a model to describe the ion population of a 3D unmagnetised plasma has been presented. A velocity-dependent collision term has been included in the equations of motion for the ions. Finite-Larmor radius effects are retained exactly. The electron population is magnetised.

For plasma parameters relevant to the low-confinement mode of the toroidal heliac H1-NF, it has been shown that collisional effects can be important in the plasma centre. The plasma edge, however, is almost in the collisionless regime. Numerical simulations have shown that the combined effects of a negative radial field and ion-ion collisions lead to a global improvement of the ion confinement. The formation of a negative radial electric field is mainly responsible for the improvement in confinement. However, collisional effects are important near the magnetic axis; this can lead to an effective randomisation of the ion population in this region. Away from the magnetic axis the plasma is almost collisionless. Experimental measurements have shown a dramatic reduction of the fluctuation level in the high-confinement mode; this phenomenon is followed by an increase in the plasma density (Shats *et al.* 1996), which is consistent with our numerical results.

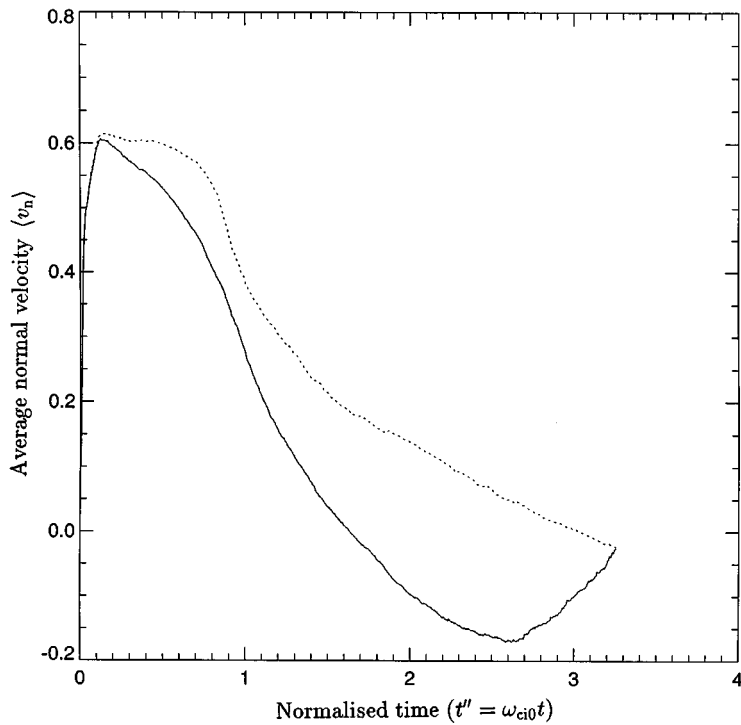


**Fig. 6.** Average normal velocity  $\langle v_n \rangle$  for the  $Ar^+$  ion population as function of the normalised time for case A (solid curve) and for case B (dotted curve).

The dramatic reduction in the fluctuation level has not been explained. It is worth pointing out that the ion collisional parameter  $\nu_{*i} \equiv \omega_{bi}/\nu_i$ , where  $\omega_{bi}$  is the ion bounce frequency and  $\nu_i$  is the effective ion collision frequency, is of the order of unity for H1-NF plasma parameters. This suggests that the ion trapping can be important. In particular the trapped-ion instability can be excited in such a plasma. However, a correct treatment of the trapped-ion instability in stellarator geometry is beyond the scope of this paper. Current theoretical research work focuses on the 3D gyro-kinetic formalism, in which collisional and trapping effects are modeled very accurately. We hope to report quantitative results in a separate paper.

### Acknowledgments

M. Shats is greatly acknowledged for providing the experimental data and for fruitful discussions. The author was supported by a Canadian NSERC research grant and by an Australian National University research grant. Numerical calculations were performed on the VPP300 Supercomputer at the Australian National University Supercomputer Facility.

## References

- Antonsen, T. M., and Lane, J. B. (1980). *Phys. Fluids* **23**, 1205.
- Braginskii, S. I. (1965). In 'Review of Plasma Physics', Vol. 1 (Consultants Bureau: New York).
- D'haeseleer, W. D., Hitchon, W. N. G., Callen, J. D., and Shohet, J. L. (1991). 'Flux Coordinates and Magnetic Field Structure' (Springer: Berlin).
- Drake, J. F., and Antonsen, T. M. (1984). *Phys. Fluids* **27**, 898.
- Frieman, E. A., and Chen, L. (1982). *Phys. Fluids* **25**, 502.
- Hazeltine, R. D. (1973). *Plasma Phys.* **15**, 77.
- Hazeltine, R. D., and Meiss, J. D. (1992). 'Plasma Confinement' (Addison-Wesley: New York).
- Hirshman, S. P., and Betancourt, O. (1991). *J. Comp. Phys.* **86**, 99.
- Hirshman, S. P., and Lee, D. K. (1986). *Comp. Phys. Commun.* **38**, 161.
- Hirshman, S. P., and Meier, H. K. (1985). *Phys. Fluids* **28**, 1387.
- Hirshman, S. P., and Whitson, J. C. (1983). *Phys. Fluids* **26**, 3553.
- Press, W. H., Flannery, B. P., Teukolsky, S. A., and Vetterling, W. T. (1983). 'Numerical Recipes in Fortran' (Cambridge University Press).
- Rewoldt, G., Tang, W. M., and Chance, M. S. (1982). *Phys. Fluids* **25**, 480.
- Shats, M. G., Rudakov, D. L., Blackwell, B. D., Borg, G. G., Dewar, R. L., Hamberger, S. M., Howard, J., and Sharp, L. E. (1996). *Phys. Rev. Lett.* **77**, 4190.
- Shats, M. G., Boswell, R. W., Rudakov, D. L., and Rudakov, L. I. (1997). Radial force balance during transitions to improved confinement mode in the H-1 heliac. *Phys. Plasmas* (to appear).
- Spitzer, L. (1956). 'The Physics of Fully Ionized Gases' (Interscience: New York).
- Trubnikov, B. A. (1965). In 'Review of Plasma Physics', Vol. 1 (Consultants Bureau: New York).